Journal of Structural Geology, Vol. 12, No. 2, pp. 267 to 272, 1990
Printed in Great Britain

0191-8141/90 $03.00+0.00

One-dimensional kinematics of stretching faults

W. D. MEANS

Department of Geological Sciences, State University of New York at Albany, 1400 Washington Avenue, Albany, NY 12222, U.S.A.

(*Received* 21 *March* 1989; *accepted in revised form* 25 *August* 1989)

Abstract—An analysis is given of the instantaneous motion and finite displacement across faults with wall-rocks that are changing length in the slip direction while slip accumulates. The main results of interest are that faults with extending or shortening wall-rocks can display slip-rate and net-slip gradients in the slip direction, and local reversal of the sense-of-slip over time. These effects depend on unequal rates of extension or shortening in the two wall-rock blocks. Where the rates of length-change are equal, the behavior more closely resembles the behavior of faults with rigid wall-rocks.

INTRODUCTION

STRETCHING faults (Means 1989) (Fig. 1) are hypothetical faults embedded in flowing rock bodies, with wall-rocks that change length in the slip-direction while slip accumulates. They may be anticipated in various flow environments in the Earth but will remain hypothetical until criteria for their recognition are developed and successfully applied to natural examples. One group of potentially useful criteria are provided by the kinematic and displacement properties of stretching faults. These are derived below for what will be called Type I stretching faults (with the same rate of length-change in both fault walls) and Type II stretching faults (with different rates of length-change in the two walls). The treatment is one-dimensional in the sense that the only motion considered is the motion of lines of particles lying in the slip-direction and in the fault-wall planes. This limited analysis is sufficient to reveal salient features of the slip-rate and displacement patterns of stretching faults.

As defined above and in Means (1989), a stretching fault is a fault inside a regionally straining rock volume, with slip-parallel stretching of the fault walls as a consequence of the regional strain-rate field. In these circumstances, fault slip and wall-rock flow are geometrically independent processes, though driven by the same remote loads.

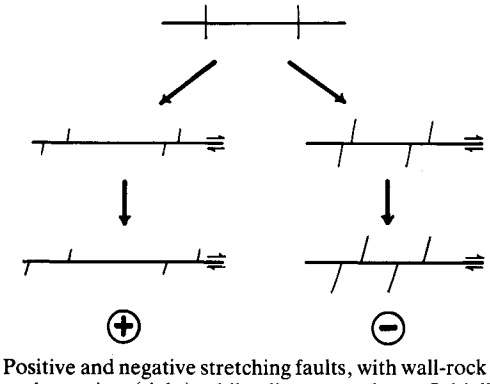

Fig. 1. Positive and negative stretching faults, with wall-rock extension (left) or shortening (right) while slip accumulates. Initially vertical lines are passive markers.

A quite different situation, and a more familiar one in the literature, is the association of fault slip and wall-rock flow where the two phenomena are geometrically coupled. Here flow occurs as a necessary accompaniment to slip, to solve room problems around obstacles like fault ramps (e.g. Rich 1934, Elliott 1976, Sanderson 1982) or arising from the existence of fault ends or 'tips' where the displacement vanishes (e.g. Elliott 1976, Hildebrand-Mittlefehldt 1979, 1980, Walsh & Watterson 1989). In these circumstances, stretching faults can still arise, but they will tend to be of the kinds referred to in Means (1989) as "half stretching faults" or "mixed stretching faults". Examples are provided, respectively, by slip-parallel extension restricted to the hangingwall at thrust ramps (e.g. Elliott 1976, fig. 2) and by the adjacent extended and shortened walls of the C-type faults of Muraoka & Kamata (1983).

In the Earth, there is probably a complete spectrum of possibilities, from faults with dominant regional, slip-independent straining of the fault walls, to faults with dominant local, slip-dependent straining of the fault walls. Faults or fault segments of intermediate character will display wall-rock strains including components of regional and of local origin. The following analysis is concerned explicitly with effects of regional wall-rock straining, remote from fault bends or ends, but the equations are general enough to have some application to cases where the wall-rock strains are locally induced.

REFERENCE FRAME AND VELOCITY EQUATIONS

The reference frame employed has its origin pinned to a particle in one fault wall and an x axis extending from this particle in the direction of slip (Fig. 2). The wall bearing the origin is arbitrarily designated the footwall.

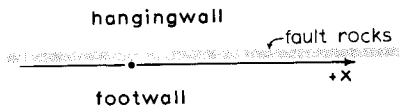

Fig. 2. Reference frame with origin fixed to a particle in the footwall plane.

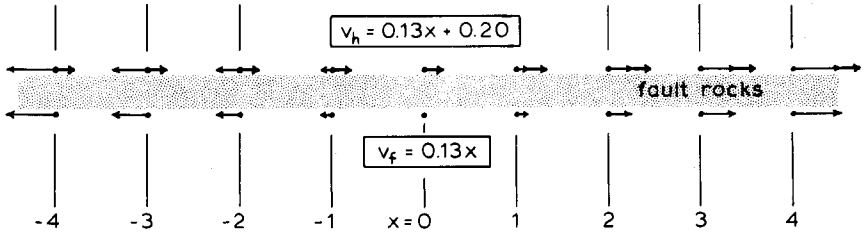

Fig. 3. Velocity field for Type I stretching fault with $a = 0.13$ per unit time and $b = 0.2$ unit distance per unit time. Heavy arrow pointing to right at each hangingwall position represents the spatially uniform component (b) of the hangingwall velocity field. Lighter arrows pointing away from the origin in both walls represent the spatially variable component (ax) of the velocity field due to the stretching. Total velocity at any hangingwall position is the vector sum of the two components. Velocity vectors drawn to the same scale as distances x.

The general *velocity equations,* which describe the velocity v of particles instantaneously at various positions x in the hangingwall h and footwall f, are

$$\begin{aligned} v_h &= cx + b \\ v_f &= ax, \end{aligned} \tag{1}$$

where a and c are the longitudinal strain-rates or *stretchings* of the footwall and hangingwall in the slip direction. If, for example, a has a value of plus $0.2t^{-1}$, the footwall is extending at a rate of 20% per unit of time. For faults with rigid wall-rocks, a and c are zero, and the velocity equations reduce to

$$\begin{aligned} v_h &= b \\ v_f &= 0. \end{aligned} \tag{2}$$

In both (1) and (2), b is the spatially uniform component of the slip-rate. In rigid fault kinematics, b is the only non-zero component of the slip-rate. In stretching fault kinematics as formulated here, b is equal to the slip-rate at the origin but elsewhere along the fault, the slip-rate is partly controlled by the stretchings a and c, as explained later.

In all the examples illustrated in this paper, a and c are both positive or both negative. These are the kinds of faults termed *positive* or *negative* stretching faults, respectively (Means 1989). Other simplifying restrictions of the analysis are that the fault trace is straight and unbranched, and that a, b and c in the velocity equations have values that are uniform over the segment of fault plane considered and constant over the interval of time considered. Finally, there is assumed no gain or loss of material along the fault plane during movement.

Faults with rigid wall-rocks, subject to the preceding restrictions, obey three rules: (1) the slip-rate is uniform along the fault trace and everywhere equal to b; (2) the net slip after any elapsed time t is also spatially uniform; and (3) this is everywhere equal to the product bt. It will be shown below that Type I stretching faults violate rule (3) and that Type II stretching faults violate all three rules of rigid fault behavior.

TYPE I STRETCHING FAULTS

Type I stretching faults are represented by velocity equations of the form

$$\begin{aligned} v_h &= ax + b \\ v_f &= ax. \end{aligned} \tag{3}$$

The velocity field of the fault walls is shown in Fig. 3, for an example with $a = 0.13$ per unit time and $b = 0.2$ unit distance per unit time.

The *slip-rate* $[v]$ of the hangingwall with respect to the footwall is given by the difference between v_h and v_f,

$$[v] = b \tag{4}$$

and is seen to be independent of position along the fault plane, in accordance with rigid fault rule (1).

The velocity equations (3) are differential equations that can be rewritten in differential form,

$$\begin{aligned} dt &= dx_h/(ax_h + b) \\ dt &= (1/a)(dx_f/x_f) \end{aligned} \tag{5}$$

and integrated to give the *position equations*

$$\begin{aligned} x_h &= (X_h + b/a)e^{at} - b/a \\ x_f &= X_f e^{at}. \end{aligned} \tag{6}$$

These give the position x_h or x_f after time t of particles, in the hangingwall and footwall, respectively, that were opposite one another at position X at time 0. The constants of integration are found by requiring that at time 0, x_h and x_f should be equal to X_h and X_f, respectively, where X_h and X_f are defined as the initial positions of hangingwall and footwall particles.

Setting X_f equal to 1 in the second equation of (6) yields the *stretch equation*

$$S = e^{at}. \tag{7}$$

This gives the stretch of each fault-wall (deformed length in the slip direction divided by undeformed length) after any elapsed time t.

The net slip NS can be found at any time t by subtracting x_f from x_h as given by (6) and is

$$NS = b/a(e^{at} - 1). \tag{8}$$

This *net-slip equation* indicates that although the slip-rate is everywhere equal to b and constant in time, the net slip is not the product of the slip-rate and t, as with rigid faults, but is greater or less than bt, depending on the stretching a. For positive stretching faults, the net slip always exceeds bt.

Notice that the velocities given by any of the velocity

equations above are velocities at fixed *positions* in space. They are only momentarily the velocities of fault-wall *particles*, since the particles are typically moving from one position to another and adopting a succession of different velocities. To obtain the *particle velocity equations*, it is necessary to differentiate the position equations (6) with respect to time, keeping X constant. This yields

$$V_h = (X_h + b/a)ae^{at}$$
$$V_f = X_f ae^{at}. \quad (9)$$

Finally, one can set equations (9) equal to each other to yield the *isovelocity distance d* with

$$d = b/a. \quad (10)$$

d gives the distance, measured from a particle in the hangingwall to a particle in the footwall, between pairs of particles that have identical velocity histories. Such pairs of particles remain separated by the same distance d as time passes, because they are always travelling at the same velocity as each other. For faults with rigid wall-rocks the isovelocity distance is effectively non-existent (equal to infinity).

Figure 4 shows three stages in the history of a Type I stretching fault, with $a = 0.13$ and $b = 0.20$ (as in Fig. 3), constructed using equations (6). No shear strain of the wall-rock blocks is indicated (i.e. the shaded regions are maintained rectangular throughout the history). This is unrealistic since the shear stress necessary for fault slip could be expected in general to promote shear strain in the wall-rock blocks. However, the magnitudes of these shear strains are undefined using the present one-dimensional analysis, and in the absence of any specified stress-state and wall-rock material properties. So the shear strain is shown as zero in Fig. 4 (and Fig. 5), in preference to showing arbitrary finite shear strains. The finite flattening normal to the fault plane *is* indicated however, assuming conservation of area in the plane of the paper. Whether or not this assumption is correct, Fig. 4 still indicates salient features of Type I faults as follows.

Both fault walls have stretched in the slip direction. At time 4 the accumulated stretch is 1.68, as equation (7) requires.

The net slip is uniform along the fault plane at each stage in the history. At time 4 the net slip is 1.05, as required by equation (8). It exceeds the product of the local slip-rate (0.2) and the time elapsed (4) by a substantial factor.

The isovelocity distance for this example is 1.54, as given by equation (10). This means that the hangingwall particle at the tip of the arrow in Fig. 4 (which is 1.54 length units from the origin) always has the same velocity as the footwall particle at the origin, namely zero. The existence of this *null velocity particle* in the hangingwall can be understood by observing that it is the particle whose velocity b to the right is exactly equalled by its velocity ax to the left due to the hangingwall stretching. Faults with rigid wall-rocks can never have null velocity particles in the wall opposite the wall to which the origin is fixed.

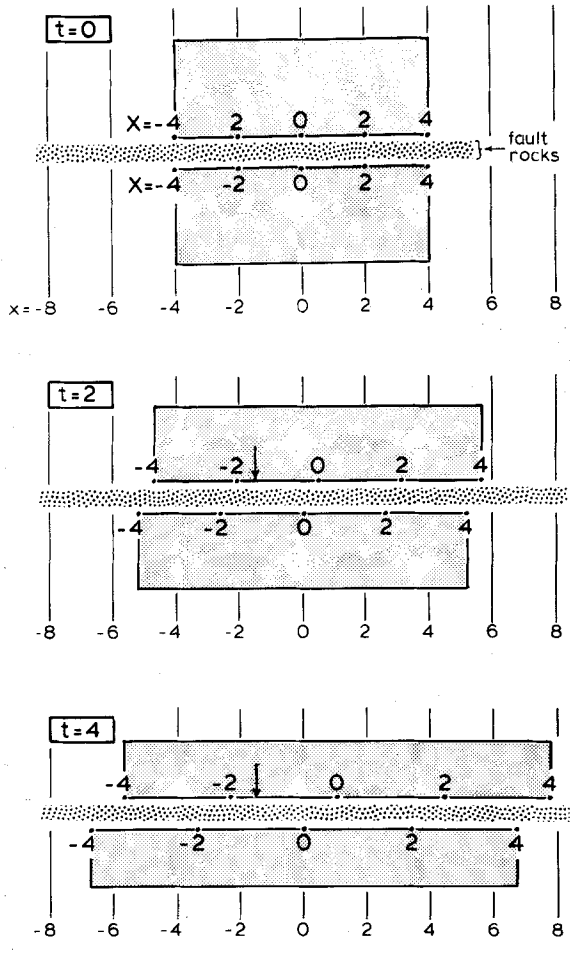

Fig. 4. Three stages in the development of a Type I stretching fault. Light numbers are spatial co-ordinates giving the distance x from the origin. Heavy numbers identify particular material particles in the fault walls according to their initial positions X. Arrow shows position of null velocity particle in the hangingwall. Note uniform net slip all along the fault.

TYPE II STRETCHING FAULTS

Equations for Type II faults are derived in similar fashion to those for Type I faults, with slightly more complex results because now the footwall and hangingwall stretchings are unequal.

The *velocity equations* are

$$v_h = cx + b$$
$$v_f = ax, \quad (11)$$

from which it can be seen that the *slip-rate equation* is

$$[v] = (c - a)x + b. \quad (12)$$

Note that the slip-rate now consists of two parts, a spatially uniform component b and a position-dependent component that varies linearly with position, by a factor which is the difference between the hangingwall and footwall stretchings. Type II faults thus always

display slip-rate gradients along the fault trace, unlike faults with rigid wall-rocks and Type I faults.

The *position equations*, obtained by integrating equations (11), are

$$x_h = (X_h + b/c)e^{ct} - b/c$$
$$x_f = X_f e^{at} \quad (13)$$

and these, by subtraction, give the *net-slip equation*

$$NS = X(e^{ct} - e^{at}) + b/c(e^{ct} - 1). \quad (14)$$

Different pairs of initially contiguous particles X thus display different net slips at any given time. Or in other words, there is always a net-slip gradient along a Type II fault.

The *particle velocity equations* are

$$V_h = (X_h + b/c)ce^{ct}$$
$$V_f = X_f a e^{at} \quad (15)$$

and an isovelocity distance d is now

$$d = b/c. \quad (16)$$

All of the equations have the same meanings as the corresponding equations for Type I faults, except for the isodistance equation. The d given in (16) applies only to the distance from a footwall particle at the *origin* to a hangingwall particle with the same (null) velocity. Other footwall particles have isovelocity partners in the hangingwall, but the distance between these pairs of particles is different from d in (16) and different for each footwall particle.

Figure 5 represents the history of a Type II fault, with a and b the same as in Fig. 4, but with the hangingwall stretching now 0.08 and thus different from the footwall stretching. Note the net-slip gradient at time 2 and time 4, indicated by the unequal separation of particle pairs 0, 2, 4, etc. There is even a reversal of the sense of the net slip somewhere between particle pairs 2 and 4 at time 4. Again, the arrow points to a null velocity particle in the hangingwall, at distance d from the origin given by (16).

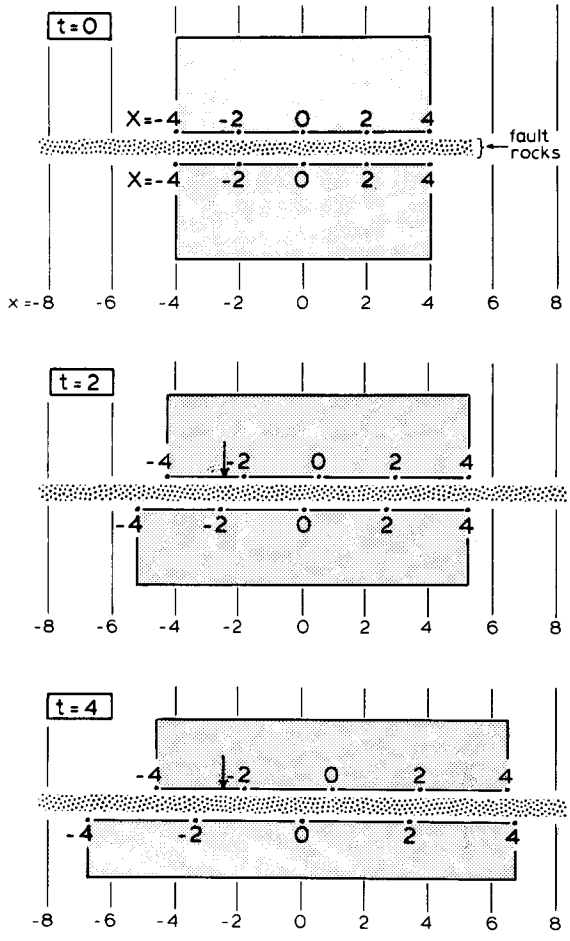

Fig. 5. Three stages in the development of a Type II stretching fault. Numbers and arrow have the same significance as in Fig. 4. Note net-slip gradient along the fault and reversal of the sense of the net slip at time 4, between particle-pairs 2 and 4.

Slip-rate and net-slip null points

Unlike rigid or Type I faults, Type II faults exhibit points where the slip-rate or the net slip are zero. The sense of the slip-rate and the net-slip reverses across these null points. Setting (12) equal to zero yields

$$x = b/(a - c) \quad (17)$$

as the position at which the slip-rate is zero. Note two important features of this *slip-rate null point*: it is fixed in position spatially but not materially. That is to say, it sits permanently at a certain distance from the origin (and from the null velocity point in the hangingwall) and material of both fault walls passes through it. At the moment of passage, the slip-rate is zero because the velocity of both fault walls is identical. In the example of Fig. 5, equation (17) indicates that the slip-rate null point is at $x = 4.0$. To the left of this point the slip-rate is always dextral; to the right it is sinistral.

The behavior of the *net-slip null point* is different. It migrates through the material of both fault walls *and* changes its position with respect to the origin. At time zero the net-slip and slip-rate null points are coincident. Thereafter the two null points separate and become more separated, spatially, as time passes.

The particle pairs X at the net-slip null point at any time t can be found by setting (14) equal to zero, yielding

$$X = (b(e^{ct} - 1))/(c(e^{at} - e^{ct})). \quad (18)$$

Thus, the net-slip null point observed earlier to lie somewhere between particles 2 and 4 at time 4 in Fig. 5, can be determined to lie precisely at the position of the particles with $X = 3.09$. The spatial position of this null point can be found by substituting $X = 3.09$ and $t = 4$ in either of the equations (13), yielding $x = 5.20$. So at time 4 in Fig. 5, the slip-rate null point is fixed at $x = 4.00$ and the net-slip null point is currently at $x = 5.20$ but migrating to the right, ever farther from the slip-rate null point as time passes.

The spatial separation of the slip-rate and net-slip null points gives rise to a segment along a Type II fault on which the senses of the slip-rate and the net slip are opposite, even with the basic slip and flow parameters a, b and c held constant. I illustrate this by considering the spatial and velocity histories of particles initially

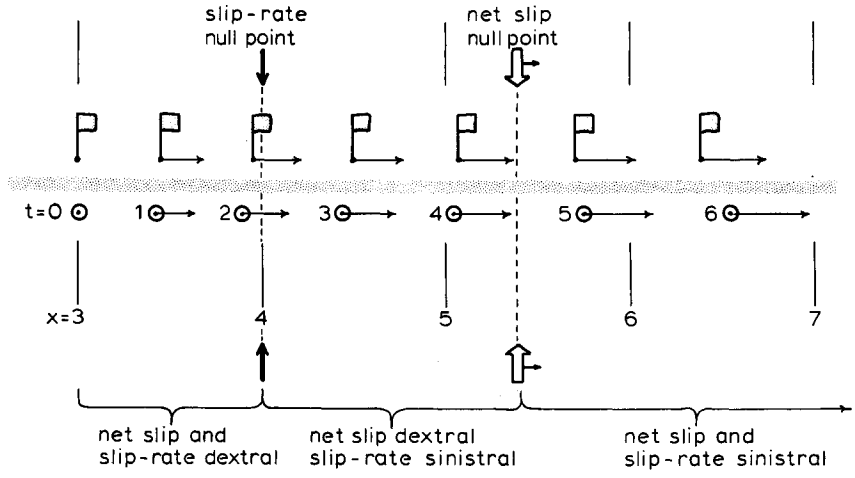

Fig. 6. History of slip for particle-pair 3 of Fig. 5, marked by circle in footwall and flag in hangingwall. Arrows indicate particle velocities at each time t. Early dextral net slip decays and becomes sinistral net-slip, as described more fully in text. The slip-rate null point is fixed at a position 4 distance units from the origin. The net-slip null point is at 5.38 distance units from the origin when the circle and the flag pass through it, but moves farther from the origin as time passes. The material of both fault walls migrates through the two null points.

opposite one another at $X = 3$ (Fig. 6). The positions of the particles at times 0–6 are calculated using equations (13) and the velocities at these positions are calculated using equations (15).

Figure 6 can be understood best if the reader imagines an observer standing on the particle $X = 3$ in the footwall throughout the history. This particle is circled in Fig. 6, and at time 0 it is at position $x = 3$. Imagine that at time 0 the observer plants a flag on the hangingwall particle immediately opposite him, also at $x = 3$. The net slip at any subsequent time, relative to the observer's post at the circle, will be the distance, measured in the slip direction, from the circle to the flag.

By time 1, the circle and the flag have both moved to the right (relative to the origin at $x = 0$) but the flag has moved farther, so the net slip is dextral. The current velocity of the flag is also slightly greater than that of the circle (0.476 units of distance per unit time vs 0.444), so the net slip is increasing. At the observer's position ($x = 3.42$), equation (12) can be used to determine that the slip-rate is positive (dextral).

By time 2 the dextral net slip has increased some and the velocity of the flag remains greater than the velocity of the circle (0.516 vs 0.505), meaning that the net slip is still instantaneously increasing. The slip-rate remains dextral, both at the observer's station and nearby at the flag.

When the flag crosses the slip-rate null point at $x = 4$, it is moving at exactly the same velocity as the particle opposite the flag in the footwall. This particle is not however the observer's particle in the footwall. When the flag's part of the fault experiences its null slip-rate moment, the observer's station is still opposite part of the fault that is slipping dextrally, though at a decreasing rate. As the observer crosses the slip rate null point, the circle and the particle opposite are instantaneously travelling at the same velocity as each other and at the same velocity as the flag was when it crossed the null point.

By time 3 the net slip is still dextral, but the circle is now travelling faster than the flag (0.576 vs 0.559), so the net slip is decreasing. The slip-rate is sinistral everywhere to the right of $x = 4$, so the sense of the slip-rate (at the circle and at the flag) is now *opposite to the sense of the net slip*. This condition persists as the circle and the flag approach the net-slip null point, with the circle catching up to the flag because its velocity is greater (0.656 vs 0.605 at time 4).

At the net-slip null point (at $x = 5.38$) the flag is once again exactly opposite the observer, and the net slip is zero. Beyond this point, the observer sees the flag moving farther and farther to his left. Sinistral net slip then accumulates indefinitely.

Note that the net-slip null point at $x = 5.38$ applies *only* to the particles initially at $X = 3$. The net-slip null point migrates to higher x values as it is crossed by particles with lower X values (initial positions). The fault segment with decreasing net slip thus widens with time.

DISCUSSION

The preceding analysis contains an arbitrary element that needs to be pointed out. I have considered a, b and c in the velocity equations (3) and (11) to be constant over whatever interval of time is considered. This is physically reasonable for a and c, since these are the fault-parallel extension-rates in the wall-rocks, and they might well be more or less constant under a given state of stress in recrystallizing wall-rocks. But setting b constant is arbitrary and was done for mathematical convenience. b is the slip-rate at the origin—i.e. the rate at which hangingwall material moves past the footwall particle to which the origin is pinned. Setting b constant brings with it the convenient feature that the slip-rate at any position x will also be constant (equation 12). But it also means that for any *particle* X other than $X = 0$, the slip-rate will vary with time. So setting b constant gives the particle at the origin a different slip-rate history from all other

particles in the footwall (constant vs varying slip-rate). I see no physical justification for this. But even if b is allowed to vary with time, the same main results are obtained for Type II faults—they exhibit slip-rate and net-slip null points, and net-slip reversal for certain particle-pairs. This also holds true if the reference frame, instead of being pinned to a particle in one fault-wall, is assigned a fixed position in a space relative to which both fault-walls are moved.

Slip-rate and net-slip gradients have been shown above to be characteristic features of Type II stretching faults but they are not diagnostic of faults with wall-rock strains of slip-independent, regional origin. Local, slip-dependent wall-rock strains due, for example, to fault end effects (e.g. Walsh & Watterson 1989) can also give rise to net-slip (and probably slip-rate) gradients, as can branching faults. So net-slip gradients alone are not sufficient evidence for positive or negative Type II stretching faults.

If large-scale stretching faults exist at all in the Earth, they are likely to be Type II. Type I are a special case, with identical stretchings in both walls, a situation not expected to be normal on large-scale faults separating rocks of different lithology. So the complex behavior indicated in Fig. 6, with the net slip increasing, then decreasing, and finally reversing sign, may be of some real importance. This net-slip reversal on faults recalls the situation encountered in flowing volumes of rock, where the shortening of a material line may increase, then decrease, and eventually reverse sign as the line recovers its original length and begins to extend, all in the course of a simple homogeneous progressive deformation (Ramberg 1959). The slip-rate and the net slip in the stretching fault case are analogous to the strain-rate and the finite strain in the case of the progressively deforming volume.

The theory outlined in this paper is for the situation where a, b and c are uniform over the length of fault plane considered. What happens when these quantities vary with position in the material, as they are likely to do in real examples? What happens if, in each small region of the material, a and c change with time? Perhaps the most worthwhile undertaking now is not to pursue these further convolutions of the theory, but to look closely at real, natural and experimental faults to see whether any of them are or were stretching faults.

Acknowledgements—This work is a by-product of research on slickensides, supported by NSF Grant EAR 860691. The paper benefitted substantially from criticism by O. A. Pfiffner, G. Oertel, S. Treagus and J. Walsh. B.-N. Ree assisted with word-processing.

REFERENCES

Elliott, D. 1976. The energy balance and deformation mechanisms of thrust sheets. *Phil. Trans. R. Soc. Lond.* **A283**, 289–312.

Hildebrand-Mittlefehldt, N. 1979. Deformation near a fault termination, Part I: a fault in a clay experiment. *Tectonophysics* **57**, 131–150.

Hildebrand-Mittlefehldt, N. 1980. Deformation near a fault termination, Part II: a normal fault in shales. *Tectonophysics* **64**, 211–234.

Means, W. D. 1989. Stretching faults. *Geology* **17**, 893–896.

Muraoka, H. & Kamata, H. 1983. Displacement distribution along minor fault traces. *J. Struct. Geol.* **5**, 483–495.

Ramberg, H. 1959. Evolution of ptygmatic folding. *Norsk geol. Tidsskr.* **39**, 99–160.

Rich, J. L. 1934. Mechanics of low-angle overthrust faulting illustrated by Cumberland thrust block, Virginia, Kentucky and Tennessee. *Bull. Am. Ass. Petrol. Geol.* **18**, 1584–1596.

Sanderson, D. J. 1982. Models of strain variation in nappes and thrust sheets. *Tectonophysics* **88**, 201–233.

Walsh, J. J. & Watterson, J. 1989. Displacement gradients on fault surfaces. *J. Struct. Geol.* **11**, 307–316.